THE JOURNAL OF PHYSICAL CHEMISTRY B

Article

pubs.acs.org/JPCB

Influence of Phospholipid Composition on Self-Assembly and Energy-Transfer Efficiency in Networks of Light-Harvesting 2 Complexes

Ayumi Sumino,[†,∥] Takehisa Dewa,*[,†,‡] Tomoyasu Noji,[†] Yuki Nakano,[†] Natsuko Watanabe,[†] Richard Hildner,[§] Nils Bösch,[§] Jürgen Köhler,[§] and Mamoru Nango*[,†]

[†]Department of Frontier Materials, Graduate School of Engineering, Nagoya Institute of Technology, Gokiso-cho, Showa-ku, Nagoya 466-8555, Japan

[‡]PRESTO, Japan Science and Technology Agency, 4-1-8 Honcho Kawaguchi, Saitama 332-0012, Japan

[§]Experimental Physics IV and BIMF, University of Bayreuth, D-95440 Bayreuth, Germany

Supporting Information

ABSTRACT: In the photosynthetic membrane of purple bacteria networks of light-harvesting 2 (LH2) complexes capture the sunlight and transfer the excitation energy. In order to investigate the mutual relationship between the supramolecular organization of the pigment−protein complexes and their biological function, the LH2 complexes were reconstituted into three types of phospholipid membranes, consisting of L-α-phosphatidylglycerol (PG), L-α-phosphatidylcholine (PC), and L-α-phosphatidylethanolamine (PE)/PG/cardiolipin (CL). Atomic force microscopy (AFM) revealed that the type of phospholipids had a crucial influence on the clustering tendency of the LH2 complexes increased from PG over PC to PE/PG/CL, where the LH2 complexes formed large, densely packed clusters. Time-resolved spectroscopy uncovered a strong quenching of the LH2 fluorescence that is ascribed to singlet−singlet and singlet−triplet annihilation by an efficient energy transfer between the LH2 complexes in the artificial membrane systems. Quantitative analysis reveals that the intercomplex energy transfer efficiency varies strongly as a function of the morphology of the nanostructure, namely in the order PE/PG/CL > PC > PG, which is in line with the clustering tendency of LH2 observed by AFM. These results suggest a strong influence of the phospholipids on the self-assembly of LH2 complexes into networks and concomitantly on the intercomplex energy transfer efficiency.

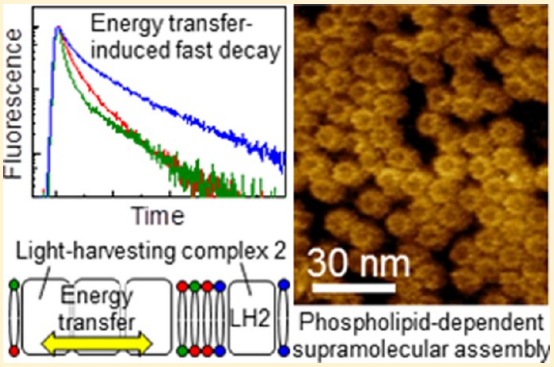

INTRODUCTION

Cell membranes consist of heterogeneously arranged proteins and lipids, and their interactions play an important role in biological activity.[1−8] In photosynthetic membranes, the proteins of the light-harvesting machinery are densely packed in lipid bilayers.[9,10] These membranes represent sophisticated photovoltaic devices for light capture and subsequent conversion of the excitation energy into an electrochemical potential.[11] In photosynthetic purple bacteria light is absorbed by a network of peripheral pigment−protein complexes (LH2) that surround the core complex (LH1-RC) where the light energy is used to create a stable charge-separated state.[12,13] The LH complexes consist of pigments [bacteriochlorophylls (BChl) and carotenoids (Car)] that are noncovalently bound by a protein scaffold that ensures their mutual arrangement. The supramolecular organization of the membranes has been studied by atomic force microscopy (AFM) and revealed a polymorphic LH2/LH1-RC organization for the various species of purple bacteria.[14] For example, in *Rhodobacter sphaeroides* dimerized LH1-RC arrays are connected by domains of LH2,[15] whereas for *Rhodospirillum photometricum*[16] and *Rhodopseudomonas palustris* hexagonally packed, paracrystalline clusters of LH2 and LH1-RC have been found.[17] Whether these variations are related to the biological function is unclear to date.

For *Rps. palustris*[17] and *Rb. sphaeroides* (LH2-only mutant)[10] AFM has shown that the membranes are phase-separated into domains composed of protein clusters and plain lipids. This suggests that the phospholipids might play an important role in the membrane organization. However, there are conflicting reports concerning this issue. Olsen et al. have found lipid molecules between LH2 complexes in *Rb. sphaeroides*,[10] whereas Gonçalves et al. have observed densely packed assemblies without lipid molecules between LH2 clusters in *Phaeospirillum molischianum*.[9] This indicates that either the lipid−protein interactions or the lipophobic interactions are involved in the assembly of the LH2 network.

There are many examples of structural and spectroscopic studies on LH2 reconstituted into phospholipid bilayers,[18−22]

Received: May 15, 2013
Revised: July 7, 2013
Published: August 6, 2013

in addition to studies of the photophysical properties of LH2 confined in mesoporous materials.[23,24] However, little is known regarding the effect of the phospholipids on the supramolecular organization of photosynthetic membranes and its tendency to form clusters, its packing density, its crystal structure, and its miscibility in the bilayers. Until now, only protein shape and size have been considered in studies of the supramolecular organization of LH2/LH1-RC in photosynthetic membranes.[25] Yet, understanding the lipid−protein interactions is important in order to control the nanostructuring of the reconstituted membranes. It is known that the supramolecular organization reacts on the light conditions during photosynthetic growth, which becomes significantly modified with respect to the organization of the photosynthetic units[16,26] as well as their phospholipid composition.[27]

In this study, we have reconstituted LH2 complexes from *Rps. acidophila* 10050 into phospholipid membranes and studied their clustering behavior by AFM and time-resolved spectroscopy as a function of the lipid composition. This LH2 complex consists of nine $\alpha\beta$ pairs of α-helical polypeptides, 27 BChl*a* (9 B800 and 18 B850 chromophores), and 18 Car, forming a nine-membered cylindrical complex (~5.5 nm in height and 8.0 nm in diameter).[12] When light is absorbed by the B800 molecules, the excitation energy is transferred on a picosecond time scale to the B850 manifold where excitonic effects play an important role.[28] Subsequently, the excitation energy is transferred between the B850 manifolds of neighboring LH2 complexes (at 5 ps),[29] and funneled to the LH1-RC (at 3−5 ps from LH2 to LH1[30] and 35 ps from LH1 to RC[31,32]). Excess energy is dissipated by singlet−singlet (S−S) and singlet−triplet (S−T) annihilation.[33] Hence, the distribution of the excitation energy within an array of LH2 complexes is sensitive to the number of singlet and triplet excitations in the cluster, which both can be controlled experimentally by the excitation density and the repetition rate of a pulsed excitation. This idea has been applied by Pflock et al., who studied homoarrays of LH2 reconstituted into lipid bilayers.[18,34,35] Combining the experimental results with dynamic Monte Carlo simulations allowed them to unravel the competition between intercomplex excitation energy transfer and annihilation.[18]

Here, we have studied the variations of the fluorescence lifetimes of LH2 as a function of the type of phospholipids. In addition, the supramolecular arrangement of the LH2 clusters was monitored by AFM. We found that the three phospholipid systems used in this study formed distinguishable LH2 nanostructures. The phospholipids lie between LH2 molecules, suggesting that they may modulate the assembly of the nanostructure of LH2. Fluorescence spectroscopy showed characteristic, nanostructure-dependent annihilation, reflecting the extent of intermolecular energy transfer in LH2 clusters. The findings of this study indicate that phospholipids modulate both the nanostructure and the function of LH2 clusters.

MATERIALS AND METHODS

Materials. Unless stated otherwise, all chemicals and reagents were obtained commercially and used without further purification. L-α-Phosphatidylcholine (egg yolk; PC) and L-α-phosphatidylglycerol (egg yolk; PG) were gifted by Nippon Fine Chemical, Co., Ltd. L-α-Phosphatidylethanolamine (*Escherichia coli*; PE), PG (*E. coli*), and cardiolipin (*E. coli*; CL) were purchased from Avanti Polar Lipids, Inc. Phospholipid constituents used in this study were PC (egg yolk) only, PG (egg yolk) only, and PE/PG/CL (*E. coli*) mixture (2/1/1, w/w/w). This lipid composition mimics that of a bacterial photosynthetic membrane.[36] In this study, these three types of phospholipid membranes are referred to as PG, PC, and PE/PG/CL. Detergents used were *n*-octyl-β-D-glucopyranoside (OG) and *N*,*N*-dimethyldodecylamine-*N*-oxide (LDAO). LH2 was isolated from *Rps. acidophila* 10500 as previously described.[37]

Reconstitution of LH2 into Lipid Bilayers. Phospholipids were dissolved in chloroform, and the solvent was evaporated under a nitrogen stream. The resulting lipid film was dried in vacuo for at least 6 h. The thin lipid film was hydrated in a Tris·HCl buffer (20 mM, pH 8.2), giving multilamellar vesicle suspension. OG solution was added to the suspension at a final concentration of 0.78 wt % to give a comicellar solution. Next, to the solution, an LH2-containing TL buffer (0.1 vol % LDAO in 20 mM Tris·HCl buffer, pH 8.2) was added in a range of 50/1−5000/1 of the lipid/protein ratio (mol/mol). The detergent was removed by dialysis for at least 24 h at 4 °C.[38,39] For calculation of the lipid/protein ratios, one CL molecule was considered as two molecules since CL is a quasi-dimerized PG. Sucrose density gradient centrifugation showed that all LH2 molecules were incorporated into liposomes. Dynamic light scattering analysis indicated that the diameter of proteoliposomes was in the range 50−200 nm. The structural integrity of LH2 was examined by absorption spectroscopy before and after reconstitution. The solutions with the B850/B800 absorbance ratio below 1.5 were used.[40] Absorption spectra of the detergent-solubilized and membrane-embedded LH2 are summarized in Figure S1 in the Supporting Information.

AFM of LH2 in Reconstituted Lipid Bilayers. Proteoliposome solution was placed on a freshly cleaved mica surface and $MgCl_2$ solution was added. The bilayers were absorbed on the mica surface via Mg^{2+}, resulting in partially formed planar lipid bilayers.[41,42] After ~1 h of incubation, the solution was gently replaced with Milli-Q water as a recording solution. Images were taken with a Picoplus 5500 (Molecular Imaging) using AAC mode, at room temperature. Cantilevers used were BL-AC40TS (OLYMPUS) whose tip radius and spring constant were approximately 10 nm and 0.1 N/m, respectively. All images were recorded under aqueous conditions in a liquid cell.

Steady-State and Time-Resolved Fluorescence Spectroscopy. LH2-reconstituted liposomal solutions were subjected to fluorescence spectroscopy at room temperature. The concentration of LH2 in all sample solutions for fluorescence measurements were adjusted to an optical density of 0.1 in the B850 absorption band. Steady-state fluorescence spectra were obtained using a spectrometer with a CCD detector (Spec-10, 100BR/LN; Roper Scientific), monochromators (SP-150 M for excitation and SP-306 for emission; Acton Research Co.), and a lamp house (tungsten halogen light source, TS-428DC; Acton Research Co.).[38,39,41] All data were obtained at room temperature, with excitation at 800 nm and an exposure time of 4 s. For the time-resolved experiments we used a pulsed Ti:sapphire oscillator pumped by a frequency-doubled Nd:YVO_4 laser (Tsunami and Millennia Xs, Spectra Physics) as excitation source.[35] The excitation wavelength was 800 nm, and the pulse duration was about 3.5 ps. The repetition rate was varied from 81 MHz to 8, 2, and 0.05 MHz by a pulse picker unit (3980, Spectra Physics). The sample was filled in a home-built rotation cell that was spun at a frequency of 30 Hz

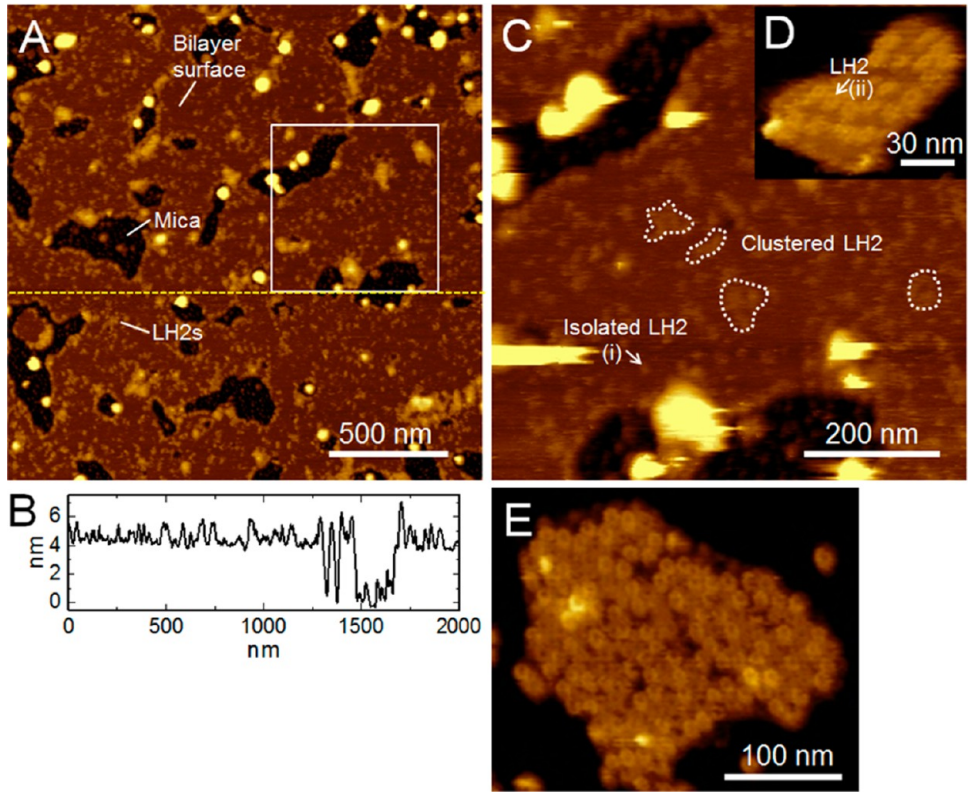

Figure 1. AFM images of LH2-reconstituted PG membranes at (A) low, (C) medium, and (D, E) high magnification. (B) is the height profile along the yellow dashed line in (A). (C) is the magnified image of the square area within the white solid line in (A). Small clusters of LH2 are enclosed by the white dotted lines in (C). (D) is a magnified image of a LH2 cluster. The lipid/protein ratio (mol/mol) was 500/1 for (A)−(D) and 50/1 for (E). All images were acquired under aqueous conditions [Milli-Q for (A), (C), and (E); 20 mM Tris·HCl, pH 8.2, for (D)] using ac-mode AFM. Scale bars: (A) 500, (C) 200, (D) 30, and (E) 100 nm.

to avoid irreversible photodegradation. The fluorescence from the sample was collected at a right angle with respect to the direction of the excitation light. The signal was spectrally dispersed using an imaging spectrograph (250 IS, Bruker), providing a spectral resolution of 3 nm in the spectral range between 830 and 990 nm. The detector was a streak camera system operated in single-sweep mode (C5680, Hamamatsu Photonics) in combination with a CCD camera (Orca-ER C4752, Hamamatsu Photonics). In all experiments, the time range was 5 ns, providing an instrument response time of 120 ps (fwhm). The fluorescence decays were recorded with photon fluences per pulse that were adjusted to 3.3×10^{12}, 6.5×10^{12}, 13×10^{12}, and 26×10^{12} photons/cm^2 per pulse incident onto the sample. To analyze the fluorescence decay curves, we spectrally integrated the streak data from 840 to 940 nm and used a 1/e time (i.e., the time required for the intensity to decay to 1/e of its maximum value) to characterize the fluorescence lifetime. All 1/e time points were obtained taking into account the width of the instrument response function. We also verified that the fluorescence decay times do not depend on the emission wavelength.

RESULTS

Self-Assembled Nanostructure of LH2 in Reconstituted Bilayers. We performed AFM studies to examine the influence of the lipid bilayer composition on the self-assembled nanostructure of LH2. The phospholipids used in this study were L-α-phosphatidylcholine (PC, egg yolk) only, L-α-phosphatidylglycerol (PG, egg yolk) only, and a ternary system comprising phosphatidylethanolamine (PE)/PG/cardiolipin (CL) [*E. coli*, 2/1/1 (w/w/w)]. This latter composition mimicked the components of bacterial photosynthetic membranes.[36] Hereafter, these phospholipid membranes are referred to as PG, PC, and PE/PG/CL, respectively.

Figure 1A,C,D shows AFM images of LH2-reconstituted PG membranes at the lipid/protein ratio = 500/1 (mol/mol). The low-magnification image (Figure 1A) and height profile (Figure 1B) along the yellow dashed line in Figure 1A indicate the formation of a single planar bilayer (4 nm in height). The protrusion from the bilayer surface is approximately 1.5 nm, similar to that reported for the extramembranous region of the periplasmic side of LH2 reconstituted into the membrane.[19] The image taken at medium magnification (Figure 1C) shows the distribution of LH2 complexes in the membrane. The white arrow and dotted lines indicate isolated and clustered LH2 complexes, respectively. This image shows that, in PG membranes, LH2 distributes as either isolated complexes or aggregates that form small clusters with sizes of approximately 30×50 nm^2 (Figure 1D), which comprise approximately 30 LH2 complexes. The center-to-center distances of nearest-neighbor LH2 complexes indicated by arrows (i) and (ii) in Figure 1C,D are approximately 50.0 nm (isolated) and 9.0 nm (clustered), respectively. While isolated LH2 complexes are diffusible within the membrane, dynamic aspects of LH2 cluster involving formation and dissociation of clusters were not observed during over 1 h observation. When the lipid/protein ratio is decreased to 50/1 (mol/mol) (i.e., the LH2 content in the membrane is increased), a large cluster of densely packed

dx.doi.org/10.1021/jp4047819 | J. Phys. Chem. B 2013, 117, 10395−10404

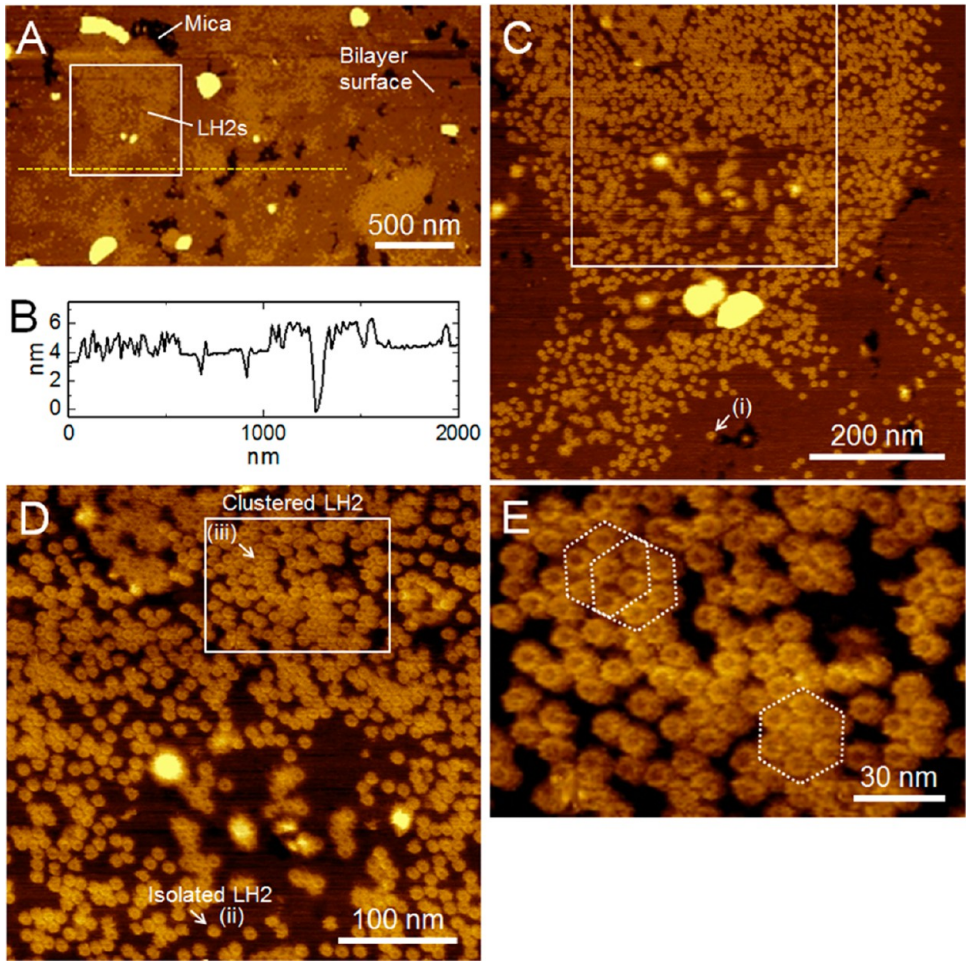

Figure 2. AFM images of LH2-reconstituted PC membranes at (A) low, (C) medium, and (D, E) high magnification. (B) is the height profile along the yellow dashed line in (A). (C) and (D) are the magnified images of the square areas within the white solid line in (A) and (C), respectively. (E) is the magnified image of the square area in (D). Hexagonally packed LH2 complexes are encircled by white dotted lines. The lipid/protein ratio was 500/1 (mol/mol). All images were acquired under aqueous conditions (Milli-Q) using ac-mode AFM. Scale bars: (A) 500, (C) 200, (D) 100, and (E) 30 nm.

LH2 complexes is observed (Figure 1E). This indicates that the cluster size depends on the lipid/protein ratio in the PG membrane.

Figure 2 shows AFM images of LH2-reconstituted PC membranes at the lipid/protein ratio = 500/1. The low-magnification image (Figure 2A) and the height profile (Figure 2B) along the yellow dashed line in Figure 2A indicate a single planar bilayer (4 nm in height) and a protrusion from the bilayer surface (~1.5 nm), similar to that observed in PG membranes. The medium- and high-magnification images (Figures 2C–E) show the organization of LH2 complexes in the bilayer; clustered (white rectangle in Figure 2D) and isolated [white arrows (i) and (ii) in Figure 2C,D] LH2 complexes coexist. The clusters are significantly larger than those in PG membranes and contain more than 100 LH2 complexes. Hexagonally packed regions are also observed (dotted hexagons in Figure 2E). The LH2 complexes distribute much more heterogeneously in PC membranes than in PG membranes. The center-to-center distances of nearest-neighbor LH2 complexes, which are indicated by arrows [(i) in Figure 2C, (ii) and (iii) in Figure 2D], are 52.3, 20.6, and 9.4 nm, respectively. The protrusion of the LH2 complexes from the membrane surface is uniform (with a height of 1.5 nm), which suggests that the LH2 complexes are assembled with their periplasmic side oriented upward. The uniform orientation may result from the spontaneous curvature of LH2, which orients LH2 in the vesicular membrane. This finding is in contrast to that in a study by Scheuring et al., who reported AFM images of a two-dimensional crystal of LH2 complexes in a 1,2-dimyristoyl-*sn*-glycero-3-phosphocholine (DMPC)/CL mixture. These arrays featured a height difference of ~0.6 nm between neighboring LH2 complexes, which the authors attributed to alternating orientations of LH2 with the cytoplasmic and periplasmic sides pointing upward.[19]

For PE/PG/CL membranes, the assembly of LH2 complexes into densely packed nanostructures is characteristic. Figure 3 shows AFM images of LH2-reconstituted PE/PG/CL membranes at the lipid/protein ratio = 500/1. The medium-magnification image (Figure 3A) and the height profile (Figure 3B) along the yellow dashed line in Figure 3A show an LH2-reconstituted PE/PG/CL vesicle adsorbed onto mica. This object features a particular shape with two layers (labeled as "1" and "2" in Figure 3A,B,F) and a domelike structure (labeled as "3" in Figure 3A,B,F), which results from an incomplete rupture of a reconstituted vesicle. Such partially ruptured structures are often found in vesicles with large LH2 clusters and are probably caused by the stiffness of LH2-rich domains, which hinders the transformation from a vesicle to a planar structure. Layer 1

dx.doi.org/10.1021/jp4047819 | J. Phys. Chem. B 2013, 117, 10395–10404

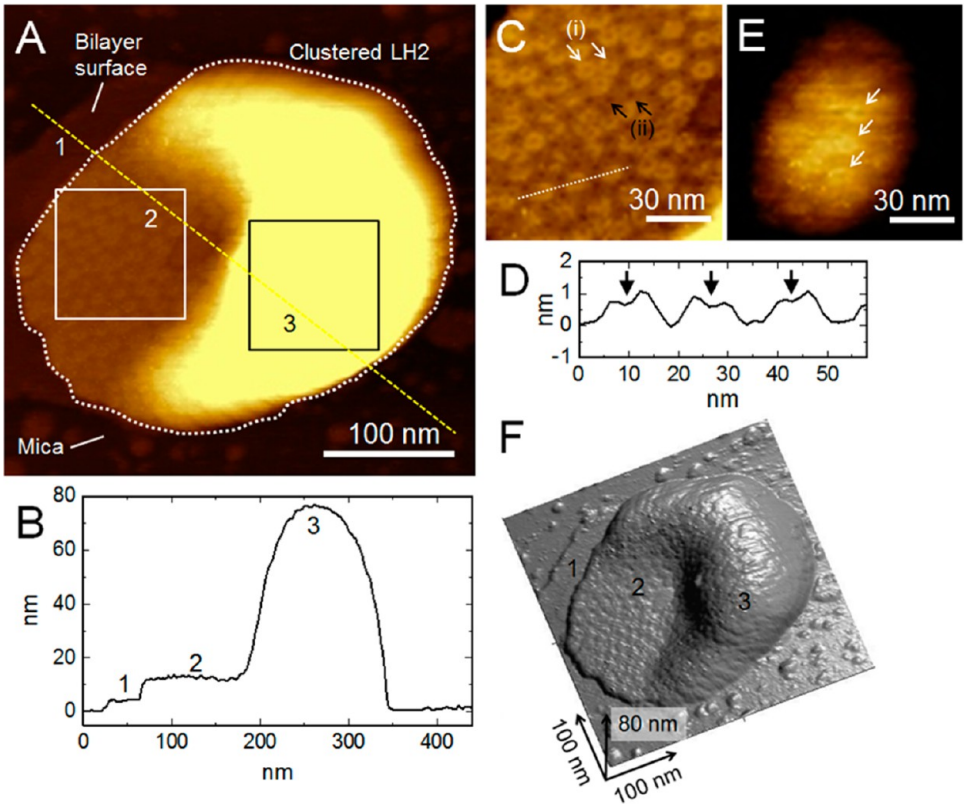

Figure 3. AFM images of LH2-reconstituted PE/PG/CL membranes at (A) medium and (C, E) high magnification. (B) is the height profile along the yellow dashed line in (A). The area of the plain bilayer at the bottom of the reconstituted architecture is indicated by "1" (in A, B, and F). The planar and domelike structures of LH2-rich clusters are indicated by "2" and "3", respectively (in A, B, and F). (C) and (E) are magnified images of the square areas enclosed by the white and black solid lines in (A), respectively. The area within the white dotted line in (A) contains large clusters of LH2 complexes. White and black arrows in (C) indicate upper and lower levels of LH2 complexes, respectively. (D) is the height profile along the white dotted line in (C). Concavities indicated by black arrows in (D) represent the central voids of three LH2 complexes at the upper level. (F) is a 3D view of (A). The lipid/protein ratio was 500/1 (mol/mol). All images were acquired under aqueous conditions (Milli-Q) in the ac-mode AFM. Scale bars: (A) 100 nm, (C, E) 30 nm, and (arrow lengths in F) 100, 100, and 80 nm.

along the yellow dashed line in Figure 3A has a height of 4 nm and is formed by a plain bilayer domain that is preferentially adsorbed onto the mica surface. This layer is followed by a partial rupture of the vesicle (layer 2, ~8 nm in height), during which two layers are formed that are stacked on top of each other. The domelike structure (layer 3) with a height of ~80 nm corresponds to the intact part of the vesicle. High-magnification images of layer 2 and the domelike area 3 are shown in parts C and E, respectively, of Figure 3. In the second layer, densely packed LH2 complexes in a two-tiered structure are observed. The upper and lower levels of LH2 complexes within this layer are indicated by white and black arrows, respectively. The height difference between the levels is 1 nm, as shown in the height profile in Figure 3D. Such a tiered structure results from a vertical displacement of LH2 that occurs during the process of vesicle–plane transformation via lateral pressure. Olsen et al. reported a displacement of 1.2 nm for a spherical cluster of LH2 complexes in a native membrane vesicle (from an LH2-only mutant of *Rb. sphaeroides*) transformed into a planar form.[10] This similarity in the displacement values suggests that the orientation of LH2 complexes in the cluster in the PE/PG/CL membrane is uniform.

Unlike the PG and PC membranes, the PE/PG/CL membrane features no isolated LH2 complexes; instead large LH2 clusters are formed. We estimate that the entire LH2 nanostructure encircled by the white dotted line in Figure 3A consists of approximately 900 LH2 complexes. In the second layer (Figure 3C), the center-to-center distances of nearest-neighbor LH2 complexes, indicated by arrows (i) and (ii) in Figure 3C, are 9.9 and 10.2 nm, respectively. In the domelike area (Figure 3E), densely packed LH2 complexes are observed, which indicates that the large LH2 cluster continuously forms over that area and over the planar second layer. Large plain bilayer patches are observed in other scan areas (data not shown). Nonbilayer lipids PE and CL form a lipid bilayer together with PG. Figure 3F is a three-dimensional image of Figure 3A.

Intermolecular Energy Transfer between LH2 Antenna Complexes. Energy-transfer kinetics between self-assembled LH2 complexes in the three membranes were characterized by (time-resolved) fluorescence spectroscopy. Figure 4A shows steady-state fluorescence spectra of LH2 in various environments upon excitation at 800 nm (black, buffer containing 0.1% *N*,*N*-dimethyldodecylamine-*N*-oxide (LDAO); blue, PG membrane; red, PC membrane; green, PE/PG/CL membrane). The spectra are centered at 867 nm in an LDAO solution and at 870 nm in the membranes with widths of 41–42 nm (full width at half-maximum, fwhm). We observe a significant quenching of fluorescence for the LH2 complexes in the membrane systems compared with that in the buffer

dx.doi.org/10.1021/jp4047819 | J. Phys. Chem. B 2013, 117, 10395–10404

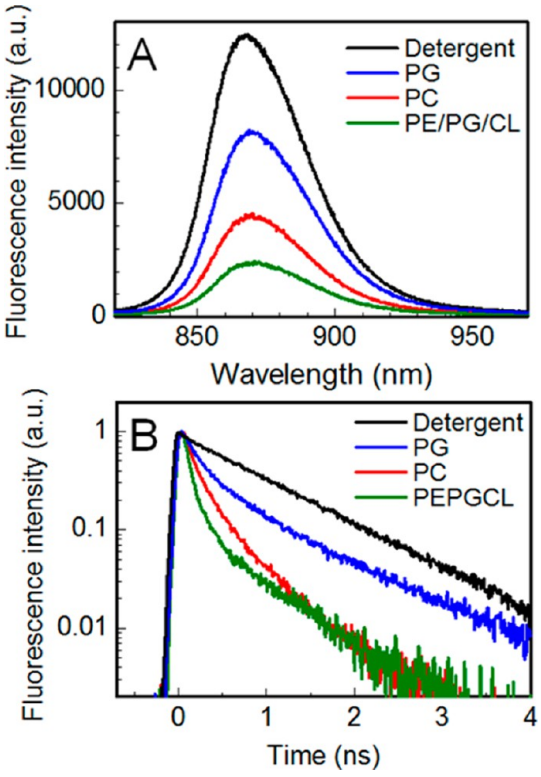

Figure 4. (A) Steady-state fluorescence spectra and (B) normalized fluorescence decays of the three LH2-reconstituted membranes. Blue, red, and green lines represent the PG, PC, and PE/PG/CL membranes, respectively. Black lines represent the spectrum and decay curve of LH2 dissolved in a buffer containing (A) 0.1% LDAO and (B) 1% octyl-β-D-glucopyranoside (β-OG), respectively. The lipid/protein ratio of the proteoliposome was 500/1 (mol/mol). The optical density of the proteoliposome solutions in the B850 band [20 mM Tris·HCl (pH 8.2)] was adjusted to 0.1. The excitation wavelength was always 800 nm. The excitation fluence and repetition rate for (B) were 26×10^{12} photons/cm^2 per pulse and 81 MHz, respectively. See the experimental details under Materials and Methods.

solution (black). The extent of quenching increases from PG to PC to PE/PG/CL.

The quenching mechanisms were further studied by time-resolved fluorescence spectroscopy using a streak camera. Since the decay kinetics do not depend on the emission wavelength, we spectrally integrate the entire emission band (from ca. 840 to 940 nm) for further analysis of the transients. Figure 4B depicts the (spectrally integrated) fluorescence decay curves recorded at a repetition rate of 81 MHz and an excitation fluence of 26×10^{12} photons/cm^2 per pulse as a function of the environment (black, buffer containing 1% β-OG; blue, PG membrane; red, PC membrane; green, PE/PG/CL membrane). The transient of LH2 in β-OG buffer is monoexponential with a decay time of 970 ps, which is in agreement with a previous study,[35] while the fluorescence decays of LH2 in the proteoliposome solutions feature strongly nonexponential kinetics with significantly shorter decay times that decrease from PG to PC to PE/PG/CL membranes. This quenching behavior is consistent with that observed in the steady-state fluorescence spectra.

To quantitatively evaluate these decay kinetics, we determined the fluorescence lifetimes of the LH2-reconstituted systems. Because these curves are clearly not monoexponential, we used a 1/e time (i.e., the time required for the intensity to decay to 1/e of its maximum value) in the following analysis. Figure 5 shows the influence of the excitation fluence (Figure

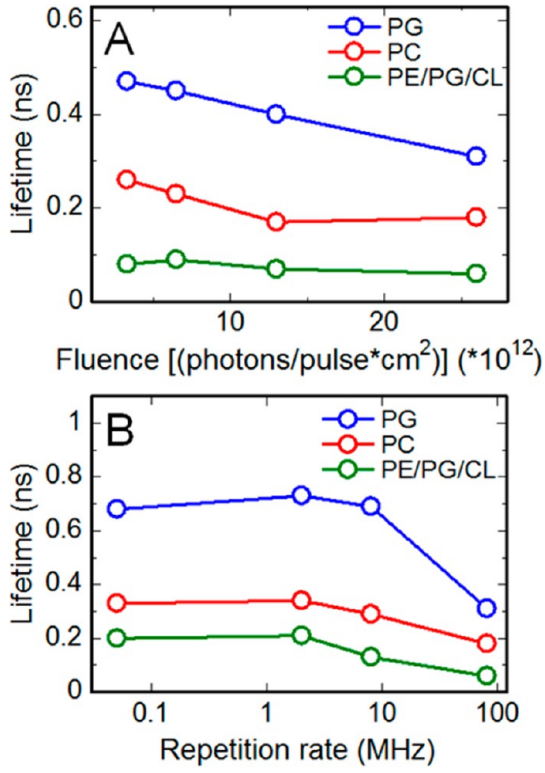

Figure 5. Lifetimes of normalized fluorescence decays of LH2-reconstituted membranes as a function of (A) the excitation fluence and (B) the repetition rate. (A) Repetition rate, 81 MHz. Excitation fluence in photons/cm^2 per pulse: 3.3×10^{12}, 6.5×10^{12}, 13×10^{12}, and 26×10^{12}. (B) Excitation fluence, 26×10^{12} photons/cm^2 per pulse. Repetition rate: 50 kHz, 2 MHz, 8 MHz, and 81 MHz. Blue, red, and green lines indicate PG, PC, and PE/PG/CL membranes, respectively. The lipid/protein ratio of proteoliposome was 500/1 (mol/mol). The optical density of proteoliposome solutions in the B850 band [20 mM Tris·HCl (pH 8.2)] was adjusted to 0.1. The excitation wavelength was 800 nm.

5A) and repetition rate (Figure 5B) on the 1/e lifetime. The general trend in these data is a decrease in the lifetime from PG to PC and PE/PG/CL. When the excitation fluence was increased at a constant repetition rate of 81 MHz, we observe a decreasing lifetime for both the LH2-reconstituted PG (Figure 5A, blue symbols) and PC membranes (red symbols). The LH2 lifetime in the PE/PG/CL membrane (green symbols) does not depend on the fluence within the experimental error. For increasing repetition rates and fixed fluences of 26×10^{12} photons/cm^2 per pulse, the lifetimes for any given environment are constant up to 2 MHz (Figure 5B) and become shorter for 8 and 81 MHz.

We also investigated the effect of the lipid/protein ratio on the relative steady-state fluorescence intensity and the lifetime (parts A and B, respectively, of Figure 6). The blue, red, and green lines represent PG, PC, and PE/PG/CL membranes, respectively, that contain LH2. The fluorescence intensity represents the maximum intensity in the steady-state spectra of LH2 in various environments, as shown, for example, in Figure 4A. These numbers are plotted relative to the fluorescence intensity of LH2 in detergent, which was normalized to 1. In

dx.doi.org/10.1021/jp4047819 | J. Phys. Chem. B 2013, 117, 10395−10404

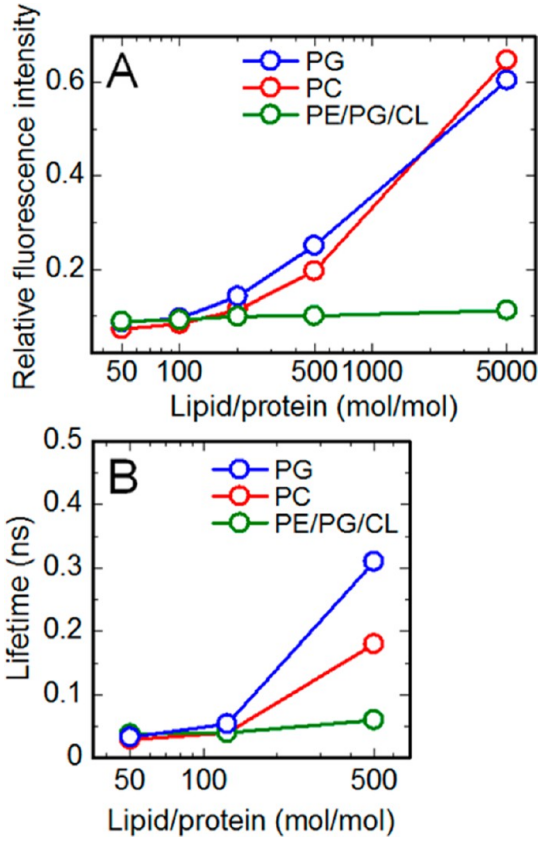

Figure 6. (A) Relative fluorescence intensity and (B) lifetime plots for the three types of LH2-reconstituted membranes as a function of the lipid/protein ratio (mol/mol). The relative fluorescence intensities and 1/e lifetimes were obtained from steady-state fluorescence spectra (Figure 4A) and normalized fluorescence decays (Figure 4B), respectively. The fluorescence intensity (A) was normalized to that observed in a TL buffer solution. Blue, red, and green lines represent PG, PC, and PE/PG/CL membranes, respectively, containing LH2. The lipid/protein ratios (mol/mol) of proteoliposome were 50/1, 100/1, 200/1, 500/1, and 5000/1 for (A) and 50/1, 125/1, and 500/1 for (B). The concentration of LH2 in all solutions was adjusted to an optical density of 0.1 in 20 mM Tris·HCl (pH 8.2). The excitation wavelength was 800 nm; the excitation fluence and repetition rate for (B) were 26×10^{12} photons/cm^2 per pulse and 81 MHz, respectively.

PG (blue) and PC (red) membranes, the relative fluorescence intensity and the lifetime increases with the lipid/protein ratio, i.e., emission quenching is reduced with decreasing protein content. In contrast, in PE/PG/CL membranes (green), fluorescence intensities and lifetimes are independent of the lipid/protein ratio and show strong quenching in the range of lipid/protein ratios investigated here.

DISCUSSION

In photosynthetic membranes, LH2 forms densely packed supramolecular clusters that involve phospholipid molecules.[9,10] Such antenna protein assemblies are considered to be required for efficient light harvesting. We found that phospholipids significantly affect the nanostructure assembly of LH2 in reconstituted membranes, thus modulating the energy-transfer efficiency between LH2 complexes. In addition, the nanostructure self-assembly of LH2 in PE/PG/CL membranes that comprised plain lipids and LH2 domains is reminiscent of the structure of native photosynthetic membranes.[9,10] In the following sections, we will discuss the details of the phospholipid-induced nanostructure and intermolecular energy transfer in such assemblies.

Relationship between the Self-Assembled Nanostructures of LH2 Complexes and Intermolecular Energy Transfer. The previously discussed AFM observations revealed the details of the self-assembled nanostructures of LH2 complexes in the phospholipid bilayers. The average center-to-center distances between neighboring LH2 complexes in the clustered regions of the three reconstituted bilayers are summarized in Table 1 and are 10.8 ± 1.9, 10.4 ± 0.9, and

Table 1. Average Distances between Neighboring LH2 Complexes in Clustered Regions of Reconstituted Membranes[a]

lipid	counts	center-to-center (nm)	edge-to-edge[b] (nm)
PG	12	10.8 ± 1.9	2.8 ± 1.9
PC	430	10.4 ± 0.9	2.4 ± 0.9
PE/PG/CL	100	9.2 ± 1.0	1.2 ± 1.0
model[c]		14.1	6.1

[a]Lipid/protein ratio was 500/1 (mol/mol). [b]Edge-to-edge distances were calculated by subtracting of the diameter of LH2 complex (8.0 nm) from the center-to-center distances. [c]Model for rough estimation of the center-to-center and edge-to-edge distances was based on a hexagonal lattice that is occupied by LH2 in a matrix of lipid bilayer at L/P = 500/1. The surface areas of the LH2 and the phospholipid were assumed to be 50 and 0.5 nm^2, respectively.

9.2 ± 1.0 nm in PG, PC, and PE/PG/CL bilayers, respectively. These numbers are consistent with the value of 9.2 ± 0.3 nm reported for the native membrane of *Rb. sphaeroides* (an LH2-only mutant).[10] If LH2 complexes are assumed to be homogeneously and hexagonally distributed in the bilayer with a lipid/protein ratio of 500, the center-to-center distance can be estimated to be 14.1 nm. This result suggests that LH2 complexes form clusters in membrane systems to a greater or lesser extent. Edge-to-edge distances were calculated by subtracting the outer diameter of LH2 (8.0 nm)[12,21] from the center-to-center distances, which yielded distances of 2.8 ± 1.9, 2.4 ± 0.9, and 1.2 ± 1.0 nm for the PG, PC, and PE/PG/CL membranes, respectively. All edge-to-edge distances are larger than the diameter of a lipid molecule (0.8 nm),[43] which indicates that (several) phospholipid molecules lie between the LH2 complexes in the clusters. These estimated edge-to-edge distances are sufficiently short to allow for efficient energy transfer between the B850 rings of neighboring LH2 complexes.[44] Notably, the orientation of LH2 in the three membrane systems is uniform, which further facilitates energy transfer. Steady-state and time-resolved spectroscopies showed that the quenching of the LH2 fluorescence becomes more efficient, i.e., the relative fluorescence intensity and lifetime decrease, when the LH2 packing density and cluster sizes increase. This clear trend is observed for PG to PC and PE/PG/CL membranes (Figures 4 and 5) and when the lipid to protein (L/P) ratio is decreased (i.e., the LH2 content in the membranes is increased, Figure 6). In a previous study, Pflock et al. showed, by combining time-resolved spectroscopy with dynamic Monte Carlo simulations on LH2 arrays of varying size and geometry, that fluorescence quenching is directly related to the LH2 cluster size. In larger LH2-clusters, more B850 singlet excitations are present, which enhances the probability of two excitations meeting on the same LH2 complex by efficient intermolecular energy transfer between

dx.doi.org/10.1021/jp4047819 | J. Phys. Chem. B 2013, 117, 10395−10404

densely packed LH2s. This enhanced probability gives rise to singlet−singlet annihilation (SSA) and accordingly quenches the fluorescence. We also find a more efficient fluorescence quenching using higher excitation fluences (Figure 5A). In a given reconstituted membrane system, i.e., for a given average cluster size, the use of higher excitation fluences increases the number of singlets per cluster, consequently leading to a greater probability of SSA.

Although SSA is the most efficient quenching process in LH2 clusters because of the short time constant (~1 ps), at high repetition rates singlet−triplet annihilation (STA) emerges as an additional quenching mechanism. A B850 singlet excited state may be deactivated, in addition to fluorescence and SSA, via intersystem crossing into a B850 triplet state, which itself is rapidly quenched via triplet−triplet energy transfer to an adjacent carotenoid (Car) molecule. Because the triplet lifetime of Car is approximately 7 μs, repetition rates greater than the inverse of this time constant give rise to a substantial accumulation of Car triplets in the clusters. When a mobile B850 singlet excitation is transferred to an LH2 complex that carries a (immobile) Car triplet excitation, the singlet excited state is annihilated, and the emission is quenched. The efficiency of annihilation (and thus of energy transfer) decreases as PE/PG/CL > PC > PG, and the LH2 cluster sizes follow the same order (decreasing as PE/PG/CL > PC > PG). This clear relationship indicates that the energy-transfer efficiency, which is related to the assembly of LH2 complexes into nanostructures, can be modulated by the phospholipid constituents.

Effect of Phospholipids on the Nanostructure of LH2. Our AFM and fluorescence spectroscopy data demonstrate that PE/PG/CL membranes facilitate the assembly of densely packed LH2 nanostructures regardless of the lipid/protein ratio, whereas for the other lipid bilayer systems, the composition and L/P ratio influence the packing densities and cluster sizes. Because the percentage of anionic phospholipids (per total lipids) varies (100, 0, and 50% in PG, PC, and PE/PG/CL membranes, respectively), we also investigated the effect of the anionic charge density on the self-assembly properties of LH2 in these membranes. If most of the LH2 clusters formed at 50% charge density, a membrane with a PG/PC ratio of 1:1 should give spectroscopic results similar to those of PE/PG/CL membranes. However, such PG/PC membranes do not show significant quenching in comparison with PE/PG/CL membranes (data not shown), which suggests that both the charge density and the phospholipid species affect the nanostructure of LH2. Russell et al. reported that PE, PC, and CL bind to purified LH2 molecules but PG does not.[27] Chandler et al. reported a simulation in which neither PE nor PG is preferentially bound to LH2 molecules.[45] Therefore, the binding of PE and/or CL to LH2 is probably involved in the formation of large self-assembled nanostructures in PE/PG/CL membranes.

The phospholipid composition of photosynthetic bacteria has been reported to be affected by changes in growth conditions, such as variations in the light intensity and in the anaerobic/aerobic environment.[27] Phospholipids could modulate the photosynthetic LH activity by changing the organization of LH2 clusters. In addition to their role as LH2-bound lipids, the phospholipids in the densely packed LH2 complexes and in the plain lipid areas in the native membrane could enhance quinone/quinol shuttling between the RC and the cytochrome bc_1 complex.[14]

The phospholipid species could play a role in the orientation of LH2 as well. AFM showed a uniform orientation of LH2 in the PE/PG/CL membranes. A previous study using PC/CL reported alternating orientations of LH2 in reconstituted two-dimensional crystals.[19] PE molecules might be one of the elements causing the uniform orientation of LH2 due to a preferable lipid−protein interaction. To clarify these issues, further investigations will be required. The formation of self-assembled structures of LH2 may result from overall interactions between lipid−lipid, lipid−protein, and protein−protein. Although it is difficult to pinpoint the exact role of phospholipids in the formation of self-assembled structures, our findings clearly demonstrate that phospholipids modulate the molecular assembly of LH2, as previously discussed. This may contribute to a better understanding of the function of the supramolecular organization of LH complexes in photosynthetic membranes.

Recently, we observed a similar phospholipid-dependent assembly of a mixed LH2/LH1-RC nanocomposite system; LH2 and LH1-RC distribute rather homogeneously in PG, whereas they form densely packed clusters in PE/PG/CL membranes.[46] LH2 and LH1-RC distribute heterogeneously in the latter membrane, where the homo pairing of LH1-RC was frequently observed. Upon the excitation of LH2 (B800), prominent quenching of LH2 and emission from LH1-RC in the PE/PG/CL membrane were observed; in contrast, in PG membranes both the quenching of LH2 and the emission from LH1-RC were less pronounced. These results also indicate that phospholipids significantly modulate the assembly structure of the LH2/LH1-RC nanocomposites and the energy-transfer activity.

Phospholipids are key elements in the structure and function of photosynthetic membranes,[9,10] which are naturally occurring "nanofactories" for light-energy conversion. The nanoarchitecture of photosynthetic membranes adapts to light intensity[16] by changing the ratio of LH2 to LH1-RC and the array of the LH2/LH1-RC assembly. The excitonic nanocomponent, LH2, adapts to the light intensity: whereas under poor photon flux it enhances light capture and energy transfer to LH1-RC via intercomplex energy transfer, under high-light conditions quenching mechanisms function to inhibit the generation of harmful singlet oxygen.[47] These sophisticated mechanisms work well in such a nanoassembly in nature. Understanding the precise nanostructure and function of the assembled excitonic and photovoltaic devices is important for us to learn how nature manages and utilizes nanotechnology. For example, it would be crucial to find a minimum size of LH2 clusters for the light-harvesting function. Our bottom-up fabrication of nanostructures is advantageous with respect to this purpose.

■ CONCLUSIONS

We demonstrated that phospholipids modulate the self-assembly of the nanostructure of LH2 and the energy transfer efficiency between LH2 complexes. This is the first study to describe the effects of phospholipid constituents on the self-assembly of the nanostructure of LH2 and its role in the intermolecular energy transfer. The formation of self-assembled structures may result from overall interactions between lipid−lipid, lipid−protein, and protein−protein. Specific phospholipids bound to LH2 could play an important role in this modulation. The quantitative analysis using time-resolved fluorescence spectroscopy revealed that the intercomplex energy-transfer efficiency varies strongly as a function of the

morphology of the self-assembled structures. These findings shed light on the roles of phospholipids in the self-assembly of membrane proteins and should improve our understanding of the light-harvesting function of photosynthetic membranes, heterogeneous membrane organization (protein clusters and plain lipid areas). Those help in the construction of artificial light-harvesting systems composed of light-harvesting complexes, which are well organized in lipid bilayers. Phospholipids are one of the key components related to the formation and function of such nanostructures.

■ ASSOCIATED CONTENT

Supporting Information

Absorption spectra of detergent-solubilized and membrane-embedded LH2. This material is available free of charge via the Internet at http://pubs.acs.org.

■ AUTHOR INFORMATION

Corresponding Authors

*Tel./fax: +81-52-735-5144. E-mail: takedewa@nitech.ac.jp.
*Tel./fax: +81-52-735-5226. E-mail: nango@nitech.ac.jp.

Present Address

[‖]Ayumi Sumino: Department of Molecular Physiology and Biophysics, Faculty of Medical Sciences, University of Fukui, Fukui 910-1193, Japan.

Notes

The authors declare no competing financial interest.

■ ACKNOWLEDGMENTS

The authors would like to thank Prof. Shigeru Itoh, Dr. Hisanori Yamakawa (Nagoya University), Dr. Masaharu Kondo (Nagoya Institute of Technology), and Dr. Tobias Pflock (University of Bayreuth) for helpful comments and discussion. The authors are grateful to Prof. Richard J. Cogdell and Dr. Alastair T. Gardiner (Glasgow University) for the gift of photosynthetic bacterial culture. This work was supported by PRESTO (Japan Science and Technology Agency, JST). M.N. and T.D. thank AOARD for funding. A.S. thanks Grant-in-Aid for JSPS Fellows (23-02697) for a fellowship. R.H., N.B., and J.K. gratefully acknowledge financial support by the German Research Foundation (DFG, GRK 1640), and the State of Bavaria within the initiative "Solar Technologies Go Hybrid".

■ ABBREVIATIONS

LH2, light-harvesting complex 2; LH1-RC, light-harvesting/reaction center complex; AFM, atomic force microscopy; PG, L-α-phosphatidylglycerol; PC, L-α-phosphatidylcholine; PE, L-α-phosphatidylethanolamine; CL, cardiolipin; *Rb.*, *Rhodobacter*; *Rsp.*, *Rhodospirillum*; *Rps.*, *Rhodopseudomonas*

■ REFERENCES

(1) Simons, K.; Toomre, D. Lipid Rafts and Signal Transduction. *Nat. Rev. Mol. Cell Biol.* **2000**, *1*, 31−39.

(2) Phillips, R.; Ursell, T.; Wiggins, P.; Sens, P. Emerging Roles for Lipids in Shaping Membrane-Protein Function. *Nature* **2009**, *459*, 379−385.

(3) Mouritsen, O. G.; Bloom, M. Mattress Model of Lipid-Protein Interactions in Membranes. *Biophys. J.* **1984**, *46*, 141−153.

(4) Bowie, J. U. Solving the Membrane Protein Folding Problem. *Nature* **2005**, *438*, 581−589.

(5) Lee, A. G. How Lipids Affect the Activities of Integral Membrane Proteins. *Biochim. Biophys. Acta* **2004**, *1666*, 62−87.

(6) Hansen, S. B.; Tao, X.; MacKinnon, R. Structural Basis of PIP2 Activation of the Classical Inward Rectifier K^+ Channel Kir2.2. *Nature* **2011**, *477*, 495−498.

(7) Caffrey, M.; Feigenson, G. W. Fluorescence Quenching in Model Membranes. 3. Relationship between Calcium Adenosinetriphosphatase Enzyme Activity and the Affinity of the Protein for Phosphatidylcholines with Different Acyl Chain Characteristics. *Biochemistry* **1981**, *20*, 1949−1961.

(8) Simmonds, A. C.; Lee, A. G. Membrane Fluidity Is Not an Important Physiological Regulator of the (Ca^{2+}-Mg^{2+})-Dependent ATPase of Sarcoplasmic Reticulum. *J. Biol. Chem.* **1984**, *259*, 8070−8071.

(9) Gonçalves, R. P.; Bernadac, A.; Sturgis, J. N.; Scheuring, S. Architecture of the Native Photosynthetic Apparatus of *Phaeospirillum molischianum*. *J. Struct. Biol.* **2005**, *152*, 221−228.

(10) Olsen, J. D.; Tucker, J. D.; Timney, J. A.; Qian, P.; Vassilev, C.; Hunter, C. N. The Organization of LH2 complexes in Membranes from *Rhodobacter sphaeroides*. *J. Biol. Chem.* **2008**, *283*, 30772−30779.

(11) Blankenship, R. E. *Molecular Mechanisms of Photosynthesis*; Blackwell Science: Oxford, 2002.

(12) McDermott, G.; Prince, S. M.; Freer, A. A.; Hawthornthwaite-Lawless, A. M.; Papiz, M. Z.; Cogdell, R. J.; Isaacs, N. W. Crystal Structure of an Integral Membrane Light-Harvesting Complex from Photosynthetic Bacteria. *Nature* **1995**, *374*, 517−521.

(13) Roszak, A. W.; Howard, T. D.; Southall, J.; Gardiner, A. T.; Law, C. J.; Isaacs, N. W.; Cogdell, R. J. Crystal Structure of the RC-LH1 Core Complex from *Rhodopseudomonas palustris*. *Science* **2003**, *302*, 1969−1972.

(14) Sturgis, J. N.; Tucker, J. D.; Olsen, J. D.; Hunter, C. N.; Niederman, R. A. Atomic Force Microscopy Studies of Native Photosynthetic Membranes. *Biochemistry* **2009**, *48*, 3679−3698.

(15) Bahatyrova, S.; Frese, R. N.; Siebert, C. A.; Olsen, J. D.; van der Werf, K. O.; van Grondelle, R.; Niederman, R. A.; Bullough, P. A.; Otto, C.; Hunter, C. N. The Native Architecture of a Photosynthetic Membrane. *Nature* **2004**, *430*, 1058−1062.

(16) Scheuring, S.; Sturgis, J. N. Chromatic Adaptation of Photosynthetic Membranes. *Science* **2005**, *309*, 484−487.

(17) Scheuring, S.; Gonçalves, R. P.; Valérie, P.; Sturgis, J. N. The Photosynthetic Apparatus of *Rhodopseudomonas palustris*: Structures and Organization. *J. Mol. Biol.* **2006**, *358*, 83−96.

(18) Pflock, T. J.; Oellerich, S.; Krapf, L.; Southall, J.; Cogdell, R. J.; Ullmann, G. M.; Köhler, J. The Electronically Excited States of LH2 Complexes from *Rhodopseudomonas acidophila* Strain 10050 Studied by Time-Resolved Spectroscopy and Dynamic Monte Carlo Simulations. II. Homo-Arrays of LH2 Complexes Reconstituted into Phospholipid Model Membranes. *J. Phys. Chem. B* **2011**, *115*, 8821−8831.

(19) Gonçalves, R. P.; Busselez, J.; Lévy, D.; Seguin, J.; Scheuring, S. Membrane Insertion of *Rhodopseudomonas acidophila* Light Harvesting Complex 2 Investigated by High Resolution AFM. *J. Struct. Biol.* **2005**, *149*, 79−86.

(20) Scheuring, S.; Seguin, J.; Marco, S.; Lévy, D.; Breyton, C.; Robert, B.; Rigaud, J.-L. AFM Characterization of Tilt and Intrinsic Flexibility of *Rhodobacter sphaeroides* Light Harvesting Complex 2 (LH2). *J. Mol. Biol.* **2003**, *325*, 569−580.

(21) Fujii, R.; Shimonaka, S.; Uchida, N.; Gardiner, A. T.; Cogdell, R. J.; Sugisaki, M.; Hashimoto, H. Construction of Hybrid Photosynthetic Units using Peripheral and Core Antennae from Two Different Species of Photosynthetic Bacteria: Detection of the Energy Transfer from Bacteriochlorophyll *a* in LH2 to Bacteriochlorophyll *b* in LH1. *Photosynth. Res.* **2008**, *95*, 327−337.

(22) Richter, M.; Baier, J.; Cogdell, R. J.; Köhler, J.; Oellerich, S. Single-Molecule Spectroscopy Characterization of Light-Harvesting 2 Complexes Reconstituted into Model Membranes. *Biophys. J.* **2007**, *93*, 183−191.

(23) Oda, I.; Hirata, K.; Watanabe, S.; Shibata, Y.; Kajino, T.; Fukushima, Y.; Iwai, S.; Itoh, S. Function of Membrane Protein in Silica Nanopores: Incorporation of Photosynthetic Light-Harvesting Protein LH2 into FSM. *J. Phys. Chem. B* **2006**, *110*, 1114−1120.

(24) Ikemoto, H.; Tubasum, S.; Pullerits, T.; Ulstrup, J.; Chi, Q. Nanoscale Confinement and Fluorescence Effects of Bacterial Light Harvesting Complex LH2 in Mesoporous Silicas. *J. Phys. Chem. C* **2013**, *117*, 2868−2878.
(25) Frese, R. N.; Pàmies, J. C.; Olsen, J. D.; Bahatyrova, S.; van der Weij-de Wit, C. D.; Aartsma, T. J.; Otto, C.; Hunter, C. N.; Frenkel, D.; van Grondelle, R. Protein Shape and Crowding Drive Domain Formation and Curvature in Biological Membranes. *Biophys. J.* **2008**, *94*, 640−647.
(26) Brotosudarmo, T.; Kunz, R.; Böhm, P.; Gardiner, A. T.; Moulisova, V.; Cogdell, R. J.; Köhler, J. Single-Molecule Spectroscopy Reveals That Individual Low-Light LH2 Complexes from *Rhodopseudomonas palustris* 2.1.6. Have a Heterogeneous Polypeptide Composition. *Biophys. J.* **2009**, *97*, 1491−1500.
(27) Russell, N. J.; Coleman, J. K.; Howard, T. D.; Johnston, E.; Cogdell, R. J. Rhodopseudomonas acidophila Strain 10050 Contains Photosynthetic LH2 Antenna Complexes That Are Not Enriched with Phosphatidylglycerol, and the Phospholipids Have a Fatty Acyl Composition That Is Unusual for Purple Non-Sulfur Bacteria. *Biochim. Biophys. Acta* **2002**, *1556*, 247−253.
(28) Shreve, A. P.; Trautman, J. K.; Frank, H. A.; Owens, T. G.; Albrecht, A. C. Femtosecond Energy-Transfer Processes in the B800-850 Light-Harvesting Complex of *Rhodobacter sphaeroides* 2.4.1. *Biochim. Biophys. Acta* **1991**, *1058*, 280−288.
(29) Agarwal, R.; Rizvi, A. H.; Prall, B. S.; Olsen, J. D.; Hunter, C. N.; Fleming, G. R. Nature of Disorder and Inter-Complex Energy Transfer in LH2 at Room Temperature: A Three Pulse Photon Echo Peak Shift Study. *J. Phys. Chem. A* **2002**, *106*, 7573−7578.
(30) Hess, S.; Chachisvilis, M.; Timpmann, K.; Jones, M.; Fowler, G.; Hunter, C.; Sundström, V. Temporally and Spectrally Resolved Subpicosecond Energy Transfer within the Peripheral Antenna Complex (LH2) and from LH2 to the Core Antenna Complex in Photosynthetic Purple Bacteria. *Proc. Natl. Acad. Sci. U. S. A.* **1995**, *92*, 12333−12337.
(31) Bergström, H.; van Grondelle, R.; Sundström, V. Characterization of Excitation Energy Trapping in Photosynthetic Purple Bacteria at 77 K. *FEBS Lett.* **1989**, *250*, 503−508.
(32) Visscher, K. J.; Bergström, H.; Sundström, V.; Hunter, C. N.; Grondelle, R. Temperature Dependence of Energy Transfer from the Long Wavelength Antenna BChl-896 to the Reaction Center in *Rhodospirillum rubrum*, *Rhodobacter sphaeroides* (w.t. and M21 Mutant) from 77 to 177K, Studied by Picosecond Absorption Spectroscopy. *Photosynth. Res.* **1989**, *22*, 211−217.
(33) Cogdell, R. J.; Gall, A.; Köhler, J. The Architecture and Function of the Light-Harvesting Apparatus of Purple Bacteria: From Single Molecules to in Vivo Membranes. *Q. Rev. Biophys.* **2006**, *39*, 227−324.
(34) Pflock, T.; Dezi, M.; Venturoli, G.; Cogdell, R. J.; Köhler, J.; Oellerich, S. Comparision of the Fluorescence Kinetics of Detergent-Solubilized and Membrane-Reconstituted LH2 Complexes from *Rhodopseudomonas acidophila* and *Rhodobacter sphaeroides*. *Photosynth. Res.* **2008**, *95*, 291−298.
(35) Pflock, T. J.; Oellerich, S.; Southall, J.; Cogdell, R. J.; Ullmann, G. M.; Köhler, J. The Electronically Excited States of LH2 Complexes from *Rhodopseudomonas acidophila* Strain 10050 Studied by Time-Resolved Spectroscopy and Dynamic Monte Carlo Simulations. I. Isolated, Non-Interacting LH2 Complexes. *J. Phys. Chem. B* **2011**, *115*, 8813−8820.
(36) Parkes-Loach, P. S.; Sprinkle, J. R.; Loach, P. A. Reconstitution of the B873 Light-Harvesting Complex of *Rhodospirillum rubrum* from the Separately Isolated α- and β-Polypeptides and Bacteriochlorophyll *a*. *Biochemistry* **1988**, *27*, 2718−2727.
(37) Papiz, M. Z.; Hawthornthwaite, A. M.; Cogdell, R. J.; Woolley, K. J.; Wightman, P. A.; Ferguson, L. A.; Lindsay, J. G. Crystallization and Characterization of Two Crystal Forms of the B800-850 Light-Harvesting Complex from *Rhodopseudomonas acidophila* Strain 10050. *J. Mol. Biol.* **1989**, *209*, 833−835.
(38) Sumino, A.; Dewa, T.; Kondo, M.; Morii, T.; Hashimoto, H.; Gardiner, A. T.; Cogdell, R. J.; Nango, M. Selective Assembly of Photosynthetic Antenna Proteins into a Domain-Structured Lipid Bilayer for the Construction of Artificial Photosynthetic Antenna Systems: Structural Analysis of the Assembly Using Surface Plasmon Resonance and Atomic Force Microscopy. *Langmuir* **2011**, *27*, 1092−1099.
(39) Sumino, A.; Dewa, T.; Takeuchi, T.; Sugiura, R.; Sasaki, N.; Misawa, N.; Tero, R.; Urisu, T.; Gardiner, A. T.; Cogdell, R. J.; Hashimoto, H.; Nango, M. Construction and Structural Analysis of Tethered Lipid Bilayer Containing Photosynthetic Antenna Proteins for Functional Analysis. *Biomacromolecules* **2011**, *12*, 2850−2858.
(40) Georgakopoulou, S.; Frese, R. N.; Johnson, E.; Koolhaas, C.; Cogdell, R. J.; van Grondelle, R.; van der Zwan, G. Absorption and CD Spectroscopy and Modeling of Various LH2 Complexes from Purple Bacteria. *Biophys. J.* **2002**, *82*, 2184−2197.
(41) Sumino, A.; Dewa, T.; Sasaki, N.; Watanabe, N.; Kondo, M.; Morii, T.; Hashimoto, H.; Nango, M. Reconstitution and AFM Observation of Photosynthetic Membrane Protein Assembly in Planar Lipid Bilayers. *e-J. Surf. Sci. Nanotechnol.* **2011**, *9*, 15−20.
(42) Seantier, B.; Kasemo, B. Influence of Mono- and Divalent Ions on the Formation of Supported Phospholipid Bilayers via Vesicle Adsorption. *Langmuir* **2009**, *25*, 5767−5772.
(43) Gennis, R. B. *Biomembranes: Molecular Structure and Function*; Springer-Verlag: New York, 1989.
(44) Noy, D.; Moser, C. C.; Dutton, P. L. Design and Engineering of Photosynthetic Light-Harvesting and Electron Transfer Using Length, Time, and Energy Scales. *Biochim. Biophys. Acta* **2006**, *1757*, 90−105.
(45) Chandler, D. E.; Gumbart, J.; Stack, J. D.; Chipot, C.; Schulten, K. Membrane Curvature Induced by Aggregates of LH2s and Monomeric LH1s. *Biophys. J.* **2009**, *97*, 2978−2984.
(46) Dewa, T.; Sumino, A.; Watanabe, N.; Noji, T.; Nango, M. Energy Transfer and Clustering of Photosynthetic Light-Harvesting Complexes in Reconstituted Lipid Membranes. *Chem. Phys.* **2013**, *419*, 200−204.
(47) Cogdell, R. J.; Howard, T. D.; Bittl, R.; Schlodder, E.; Geisenheimer, I.; Lubitz, W. How Carotenoids Protect Bacterial Photosynthesis. *Philos. Trans. R. Soc. London, B* **2000**, *355*, 1345−1349.